Angle Tracking Analysis and Test Development

R. D. Rey
DSIF Operations Section

The angle tracking systems are currently being analyzed and tests are being developed to measure their performance. This article presents the progress made on the analysis and testing of the standard 26-m-diam antenna station automatic angle tracking system. The model is discussed and certain important system constants are developed. Simulation runs of the model were performed and comparisons are made with preliminary tests performed at the Echo Deep Space Station. The article also outlines the design of the test and software processing.

I. Introduction

Efforts have been undertaken to analyze the angle tracking systems and to develop tests which will measure their performance. The overall purpose was to determine the characteristics of the 26-m automatic angle tracking system and develop a system test to assure its proper performance during operations. The test will be used for station countdown and periodic system maintenance tests.

In order to fulfill the purpose of this task a number of efforts were undertaken. First, existing test procedures were evaluated to determine whether they could be used as tests. Next, a model of the automatic angle tracking system was developed which could be analyzed and simulated. This model was used for simulating the system using the CSSL[1] III simulation program available on the Univac 1108 and for analysis of the angle error variance. Test design was performed concurrently with the above efforts and was composed of selecting those parameters which best describe the performance of the angle tracking system and to develop automated processing methods. The software development effort was also performed concurrently. This effort implemented the processing method and developed the system interface routines. As a final effort, the station countdown and periodic system maintenance test procedures will be written.

The efforts are being applied to the angle tracking systems of the standard 26-m stations, the mutual DSIF/

[1]Continuous system simulation language.

MSFN 26-m stations and the 64-m stations. Analysis and test development on the mutual station is under way and will be completed this quarter. Analysis of the 64-m antennas is beginning in this quarter. The emphasis has been on the automatic angle tracking system of the standard 26-m station. Although the task pertains to automatic angle tracking, a large amount of the analysis and tests will apply to the antenna pointing subsystem (APS) with some modifications. Also the methods and techniques developed are directly applicable to the 26-m mutual antennas and the 64-m antennas.

II. Evaluation of TD-11 and TD-12 Analysis and Software

TD-11 and TD-12 are system test descriptions for 26-m hour angle declination (HA-dec) DSN antennas. TD-11 is formally titled Angle Jitter and Boresight Shift versus Signal Level—DSIF S-Band Tracking and Communications System (DZX-1150-11-TD); while the formal title of TD-12 is Angle Tracking Bandwidth (DZX-1150-12-TD).

It was first believed that TD-11 and TD-12 could be used for testing the 26-m antenna tracking. After evaluation of these tests it was found necessary to supply analysis and new software. The purpose of this section is to discuss the results of the evaluation, i.e., the decision to develop new test software and analysis.

The TD-11 analysis and software was found to be valid. Yet, the analysis does not define the antenna error slope gain constant quantitatively. Thus, the curves of angle jitter versus signal level cannot be verified, also the use of the servo control panel bandwidth as noise bandwidth is not necessarily correct. It was decided that an angle error variance analysis would be performed in order to verify the curves and quantitatively define the parameters used.

The TD-11 software for measuring angle jitter was studied. The software is useful and offers some advantages over the new angle jitter software. The TD-11 software resides in the DIS computer. From the DIS computer it can monitor the output angle and AGC voltage. It computes the angle mean and error variance, AGC voltage mean and variance. Therefore, TD-11 will be retained as a separate test with some refinement of the analysis.

Both the TD-12 software and the analysis used to support it were found unacceptable. The analysis was based on work performed years ago. In this work the servo transfer function was derived from measured transfer functions. The coefficients determined in this manner cannot be verified analytically. Also, the coefficients of the transfer function cannot be related to parameters of the system.

The software used in TD-12 was written to calculate delay times, percent overshoots, maximum-minimum points, rise time, and settling time of a step response. These calculations were found to be correct. The program then takes a direct discrete Fourier transform of the step response to calculate the closed-loop transfer function; but the result is not the closed-loop transfer function, since the *one over s* term due to the step function has not been removed. A weakness of the program was that it takes a direct Fourier transform instead of the computationally more efficient fast Fourier transform. The program was also difficult to operate, since it resided in the DIS computer, which has no control over the angle tracking servo system.

A decision was made to perform analysis which would relate the system parameters to the performance of the system and to write a new software test program which would accurately measure the performance of the system.

III. Angle Tracking Model and Analysis

A. System Model of the Automatic Angle Tracking System

Automatic angle tracking is performed, using a two-coordinate amplitude comparison system. A four-feed horn feeds a unit of "magic T's" which are used to generate a reference channel (sum channel), hour angle (HA) and declination angle (dec) error channels. Since the two-error channels are essentially the same only the HA channel will be considered.

Shown in Fig. 1A is the basic pattern. This pattern is shifted by each feed resulting in the horn patterns (Fig. 1B). The sum of the horn pattern results in the effective antenna gain pattern of the receiver (Fig. 1C). The difference between the two patterns results in the effective antenna gain pattern of the error channel (Fig. 1D).

The received signal is coherently amplitude-detected with the reference generated by the receiver sum channel. The output of the error detector can be represented as

$$v_e(t) = \frac{K_r}{2}\sqrt{2S}\,F(\theta)\cos\phi_e + \frac{K_r}{2}\,n_{ce}(t)\cos\phi_e$$

where

$F(\theta)$ = the effective antenna gain pattern of the error channel

$\theta = \theta_r - \theta_c$ = antenna pointing error, deg

θ_r = the angle location of the object being tracked, deg

θ_c = the angle that the antenna is pointing, deg

K_r = the gain in the error channel including AGC and the multiplier gain, V/V

S = is the average received power

ϕ_e = phase-locked loop error

$n_{ce}(t)$ = gaussian white noise

If the angle error is small, then

$$F(\theta) = K_\theta\,\theta$$

where K_θ is the slope of the error pattern. The linearized error detector output is

$$v_e(t) = \frac{K_r K_\theta}{2}\sqrt{2S}\,\theta\cos\phi_e + \frac{K_r}{2}\,n_{ce}(t)\cos\phi_e$$

This equation represents the input voltage to the servo isolation amplifier whose output drives the position integrator portion of the servo electronics. The overall system model is shown in Fig. 2. In this figure $G(s)$ represents the dynamics and gains of the antenna servo system.

B. Angle Tracking Control System Model

A detailed model of the 26-m diameter angle tracking control system was developed. This model was used to define the important constants of the system, i.e., gain constants and time constants.

Shown in Fig. 3 is a functional block diagram showing the transfer gains throughout the system. Each block has associated with it a gain and a transfer function. The model is based on the assumption that the dynamics of the electronic circuitry is dominated by the integrator network and the integration of the motor. Such factors as receiver AGC, servo component dynamics, and antenna dynamics are assumed to be negligible.

The servo electronics characterize the dynamics of the antenna tracking system. A simplified schematic of the servo electronics is presented in Fig. 4. Note that this schematic represents both the high and low speed electronics which differ only in the compensation network of the preamplifier. The different networks are shown in the lower right of the figure. The resistor R_I and the capacitors C_{I1} and C_{I2} are switched to different values, depending on the BW switch position. These values and the values of the remaining components of the schematic are given in Table 1.

The transfer impedance of each amplifier feedback network is as follows:

---

1. Integrator

Off

$$A_I Z_I = A_I \frac{1 + sT_{I2}}{(1 + sT_{I1}) \times (1 + sT_{I3})}$$

$$A_I = R_{I1} + R_{I2}$$

$$T_{I1} = R_{I2}\,C_{I2}$$

$$T_{I2} = \left(\frac{R_{I1}\,R_{I2}}{R_{I1} + R_{I2}}\right)(C_{I1} + C_{I2})$$

$$T_{I3} = R_{I1}\,C_{I1}$$

On, i.e., $R_{I1} \rightarrow \infty$

$$\frac{Z_I}{B_I} = \frac{1}{sB_I}\left[\frac{1 + sT_{I2}}{1 + sT_{I1}}\right]$$

$$B_I = C_{I1}$$

$$T_{I1} = R_{I2}\,C_{I2}$$

$$T_{I2} = R_{I2}\,(C_{I1} + C_{I2})$$

$$T_{I3} \rightarrow \infty$$

2. *Low-Speed Preamplifier*

$$A_pZ_p = A_p\left(\frac{1 + sT_{p1}}{1 + sT_{p1}}\right)$$

$$A_p = 2R_{p2}$$

$$T_{p1} = \left(R_{p4} + \frac{R_{p2}}{2}\right)C_{p4}$$

$$T_{p2} = R_{p4}C_{p4}$$

3. *High-Speed Preamplifier*

$$A_pZ_p = A_p\,\frac{1 + sT_{p1}}{1 + sT_{p2}}$$

$$A_p = R_{p5}$$

$$T_{p1} = R_{p6}\,C_{p6}$$

$$T_{p2} = (R_{p5} + R_{p6})C_{p6}$$

4. *Final Amplifier*

$$A_A\,Z_A = A_A\,\frac{(1 + sT_{A1})}{(1 + sT_{A2})}$$

$$A_A = R_{A2}$$

$$T_{A1} = R_{A3}\,C_{A3}$$

$$T_{A2} = (R_{A2} + R_{A3})C_{A3}$$

The values for the transfer function constants are given in Table 2.

The gains throughout the system as shown in Fig. 5 can be defined as follows:

$$K_T = K_RK_gK_IK_p, \qquad \text{volts/sec}$$

where

K_R = gain through the receiver (K_r) and error detector (K_x) including the antenna error pattern gain (K_θ), volts/degree

K_g = signal processor gain, volts/volt

K_RK_g is adjusted to produce an input into the integrator of 5 V/degree

$K_RK_g = 5$ V/deg

The gain of the integrator (K_I) is dependent on the operating mode

Integrator off

$$K_I = \frac{R_{I1} + R_{I2}}{R_I}, \qquad \frac{\text{volts/sec}}{\text{volt}}$$

Integrator on

$$K_I = \frac{1}{R_I\,C_{I1}}, \qquad \frac{\text{volts/sec}}{\text{volt}}$$

The gain K_p accounts for the error signal fed into the preamplifier summing point which is different for the low speed and high speed modes,

Low speed

$$K_p = \frac{2\,R_{p2}}{R_{p1}}, \qquad \frac{\text{volts}}{\text{volt}}$$

High speed

$$K_p = \frac{R_{p5}}{R_{p1}}, \qquad \frac{\text{volts}}{\text{volts}}$$

The summing point is also used to feed back the rate of the output (rate feedback loop). The gain of the rate feedback is a function of the summer gain times the gain of the feedback tachometer.

Low speed

$$K_t = \left(\frac{R_{p5} + R_{p6}}{R_{p7}}\right) \times G_t, \qquad \frac{\text{volts}}{\text{rad/sec}}$$

High speed

$$K_t = \frac{R_{p5}}{R_{p1}} \times G_t, \qquad \frac{\text{volts}}{\text{rad/sec}}$$

where G_t is the tachometer gain in volts/rad/sec.

The gain of the current amplifier input summer is

$$K_A = \frac{R_{A2}}{R_{A1}}, \qquad \frac{\text{volts}}{\text{volt}}$$

The pressure valve has a linearizing feedback loop which is available only in the high-speed mode. The gain of the feedback path is,

High speed only

$$K_f = \frac{R_{A2}}{R_{A4}} \times G_f, \qquad \frac{\text{volts}}{\text{psi}}$$

where G_f is the pressure transducer gain in $\frac{\text{volts}}{\text{psi}}$

The remaining gain constants are

K_c = gain of the current amplifier

$$= \frac{1}{R_{A5}}, \qquad \frac{\text{amps}}{\text{volt}}$$

K_v = the gain of the pressure valve, psi/amp or $\frac{\text{in.}^3}{\text{amp-sec}}$

K_m = gain of the motor, $\frac{\text{rad/sec}}{\text{in.}^3}$

K_{ms} = gear ratios between the motor and the pointing axis, $\frac{\text{system radians}}{\text{motor radians}}$

The constants are important in describing the performance of the system. It was not possible to find these constants in any of the obtainable JPL specifications. But, manufacturer's specifications on the various servo components were available. Listed below are the constants calculated for use in the low-speed mode,

$$K_A = 25.6, \text{ volt/volt}$$

$$G_t = 4.4 \text{ volts/1000 rpm}$$

so that

$$K_t = \frac{2R_{p2}}{R_{p7}} \times G_t = 0.099 \times 10^{-3} \text{ volts/deg/sec}$$

$$K_c = \frac{1}{R_{A2}} = 1 \text{ mA/volt}$$

$$K_v = 0.625 \text{ gpm/mA}$$

The flow through the motor was assumed to be half the total flow due to flow in an identical drag motor. Thus, the motor constant is

$$K_m = 1500 \text{ deg/sec/gpm}$$

The gear gain is

$$K_{ms} = \frac{1}{410{,}000}$$

The constant K_T is dependent on the servo-panel gain setting (GS). For

$$GS = 0 \quad K_T = 1.5 \text{ volts/sec}$$

and

$$GS = 5 \quad K_T = 7.5$$

These values along with the time constants were used to simulate the low-speed mode using the transfer function model shown in Fig. 5.

C. Simulation Results

The transfer function model was used to simulate the response of the antenna servo system to a step input which is similar to the actual test method. Although the model is linear, it can be used to predict the ideal performance of the system.

The simulation is written in CSSL III and was run on the Univac 1108. CSSL III provides transfer functions in La Place transform plane and input functions. A step

function was used as the input. The output response of each simulation run was punched onto cards. This output was then processed by a separate processing program which yields the following:

(1) Plots of the input response, the closed-loop amplitude and phase response, and the open-loop amplitude and phase response.

(2) It prints the percent overshoot, delay time, rise time and settling of the response.

(3) It also prints the noise bandwidth, 3-dB bandwidth, and the gain and phase margins.

The processing program can accept either simulation data or test data taken by station personnel.

The simulation program and the processing program were run for four cases. The first two cases (I and II) used the actual calculated constants while the second two cases (III and IV) used a reduced motor gain in order to yield results nearer to those measured.

Results of the first two cases are presented in Table 3. The simulation shows a fast response for the system denoted by the time measurements and the relatively wide bandwidths. The gain margin and phase margin show that the system is not very stable. Runs were also made for both bandwidths using a gain setting of 10 which resulted in instability of the simulation. In Figs. 6 and 7 plots of the step function response of the system simulation are presented for the cases I and II, respectively. The response is similar to the step function response called out in JPL Spec. DOA-1146-DTL for both the 0.025 and 0.05 bandwidth switch position (the specification does not note the gain setting position). Tests performed on the actual servo control system have shown that the response is actually much slower. It was found that by lowering the motor gain (K_m) by a factor of ten, responses could be obtained which were closer to the actual servo control system responses. The simulated responses with the reduced motor gain are shown in Figs. 8 and 9 for cases III and IV. Table 4 tabulates the results from the processing program. These results are representative of the actual performance parameters which can be expected from the standard 26-m-diameter antenna automatic angle tracking system.

Also shown in Figs. 6 to 9 are the plots of the closed-loop amplitude and phase response, and the open-loop amplitude and phase response. They are presented in order to illustrate the plots which are outputted by the processing program.

IV. Angle Tracking Test Design and Results

A. Test Design and Description

The purpose of this effort was to design a test that would measure the ability of the system to track accurately with a good stability margin. It will be used to determine the angle tracking characteristics during system countdown and maintenance tests. The tests should also aid in the adjustment of the system to meet specifications. The test was designed to be used on-site by station personnel. It is easy to operate, does not require excessive time to perform and produces the results during the test so that immediate corrective action can be taken, if required.

First, parameters were chosen to measure performance which would give a good description of the system performance yet be measurable using existing station equipment. The selected parameters were:

(1) Transient responses: rise time (T_r), time delay (T_d), settling time (T_s), and percent overshoot.

(2) Transfer function: bandwidth (noise and 3 dB), phase margin and gain margin.

The APS (XDS 910) computer is used to perform the test. (Advantages of using the APS are that all stations have a computer of the proper size and that the program developed can also be used to test the computer control mode.) With the APS computer the antenna can be pointed off the collimation tower with the system in the computer control mode. As the system is switched to the automatic track mode the APS is signaled to begin taking data.

The test program samples the step response output from the datex encoders. The sample response data is stored in the computer. The computer then calculates the time domain measurements (T_r, T_d, T_s, and percent overshoot). The step response data is then differentiated and fast Fourier transformed. This results in complex samples of the closed-loop transfer function from which the amplitude response and phase response are plotted. The program then computes the 3 dB and the noise bandwidths. Next, the complex samples of the closed-loop response are used to determine the open-loop complex samples from which open-loop amplitude and phase re-

sponses are plotted. The program then calculates the phase and gain margin of the system.

B. Results of Tests Performed at DSS 12

Tests were performed at DSS 12 with preliminary software. This software contained all the main elements of the test program except the ability to begin sampling at the instantaneous beginning of the test (a minor ECO will make this capability available).

The tests were run for the same system settings that were used in case III (BW setting = 0.025, G.S. = 0) and case IV (BW setting = 0.05, G.S. = 5) of the simulation runs. Since this was a preliminary test, not all of the data was processed, although the program had the capability. Thus, only time response data and closed-loop transfer function data were plotted.

Results from the test are tabulated in Table 5. The rise time, noise bandwidth, and 3-dB bandwidth are close to the values predicted by the simulation. The numbers for percent overshoot, delay time, phase margin and gain margin were not as close. There are two possible reasons for the discrepancy. First, there is an error in detecting the beginning of the test. This error could be as large as five seconds. Second, the antenna exhibits a large amount of friction or sticking. The effect that this has on the system can be seen by studying the time response shown in Fig. 10. The response is flattened and damped greater than the simulation results.

Shown in Fig. 11 is the closed-loop transfer function of the DSS 12 servo system for the two test cases. Both curves have somewhat periodic components on the lower end. These components could be due to the sticking of the antenna or possibly could be caused by quantization errors in the sampling routine or differentiation routine.

V. Summary

A model has been developed which can be used to predict the ideal performance of the automatic angle tracking system. Parameters such as the important time constants and gains have been documented. Test software has been developed and tested at DSS 12. This software is being modified for use in standard 26- and 64-m computer control mode tests and for 26-m mutual site tests. System test procedures are currently being developed.

Future plans are to obtain test data from each station. The test data will be processed, and the results of each station will be compared with each other and with the model. These comparisons will be used to set specifications on the system. They may also be used to detect and fix anomalies between the systems. The capability of measuring angle error variance and the error coefficients will also be available.

Table 1. Servo electronics component values

Integrator network						
	Low speed			High speed		
BW switch	0.025	0.05	0.1	0.2	0.4	0.6
R_I	0.1 MΩ	0.1 MΩ	0.1 MΩ	0.133 MΩ	0.133 MΩ	0.1
R_G	0 → 1 MΩ	0 → 1 MΩ	0 → 1 MΩ	0 → 1 MΩ	0 → 1 MΩ	0 → 1 MΩ
R_{I1}	[a]					
C_{I1}	8 μF	4 μF	2 μF	1.46 μF	0.69 μF	0.47 μF
R_{I2}	2.6 MΩ	2.6 MΩ	2.6 MΩ	2.6 MΩ	2.6 MΩ	2.6 MΩ
C_{I2}	1.76 μF	0.94 μF	0.47 μF	0.72 μF	0.57 μF	0.1 μF

[a] R_{I1} = 10kΩ with integrator off
= ∞ with integrator on, series switch open

Preamplifier compensation				
Low speed R_{p1} = 84 kΩ C_{p4} = 0.45 μF	R_{p2} = 100 kΩ	R_{p3} = 100 kΩ	R_{p4} = 6.2 kΩ	R_{p7} = 1.5 MΩ
High speed R_{p1} = 144 KΩ C_{p6} = 0.37 μF	R_{p5} = 3.9 MΩ	R_{p6} = 430 KΩ	R_{p7} = 10 MΩ	
Final amplifier				
R_{A1} = 39 kΩ C_{A3} = 1.50 F	R_{A2} = 1 MΩ	R_{A3} = 100 kΩ	R_{A4} = 5 MΩ	R_{A5} = 1
High-speed pressure feedback (high speed only)				
R_V = 0 → 50 kΩ	R_{V1} = 1 MΩ	R_{V2} = 1 MΩ		

Table 2. Transfer function constants

Integrator (low-speed) constants			
0.025 BW Integrator off $A_I = 2.6 \times 10^6$	$T_{I1} = 4.576$ sec $f_{I1} = 0.0348$ Hz	$T_{I2} = 97.6 \times 10^{-3}$ $f_{I2} = 1.63151$	$T_{I3} = 80 \times 10^{-3}$ $f_{I3} = 1.990$
Integrator on $C_{I1} = 8\ \mu F$	$T_{I1} = 4.576$ sec $f_{I1} = 0.0348$ Hz	$T_{I2} = 25.376$ $f_{I2} = 0.00628$	$T_{J3} \rightarrow \infty$ $f_{J3} \rightarrow 0$
0.05 BW Integrator off $A_I = 2.6 \times 10^6$	$T_{I1} = 2.44$ sec $f_{I1} = 0.06526$ Hz	$T_{I2} = 49.4 \times 10^{-3}$ $f_{I2} = 3.249$	$T_{I3} = 4.0 \times 10^{-3}$ $f_{I3} = 3.98$
Integrator on $C_{I1} = 4\ \mu F$	$T_{I1} = 2.44$ sec $f_{I1} = 0.0653$ Hz	$T_{I2} = 10.4$ $f_{I2} = 0.01531$	$T_{I3} \rightarrow \infty$ $f_{I3} \rightarrow 0$
0.1 BW Integrator off $A_I = 2.6 \times 10^6$	$T_{I1} = 1.222$ sec $f_{I1} = 0.13052$ Hz	$T_{I2} = 24.7 \times 10^{-3}$ $f_{I2} = 6.446$	$T_{I3} = 20 \times 10^{-3}$ $f_{I3} = 7.961$
Integrator on $C_{I1} = 2\ \mu F$	$T_{I1} = 1.222$ $f_{I1} = 0.13031$	$T_{I2} = 6.47$ $f_{I2} = 0.0246$	$T_{I3} \rightarrow \infty$ $f_{I3} \rightarrow 0$
Low-speed preamplifier			
$A_p = 168 \times 10^3$	$T_{p1} = 21.690 \times 10^{-3}$ sec $f_{p1} = 7.338$ Hz		$T_{p2} = 2.79 \times 10^{-3}$ $f_{p2} = 57.$

Table 2 (contd)

Integrator (high speed) constants			
0.2 BW Integrator off $A_I = 2.6 \times 10^6$	$T_{I1} = 1.872$ sec $f_{I1} = 0.08506$ Hz	$T_{I2} = 22.8 \times 10^{-3}$ $f_{I2} = 6.984$	$T_{I3} = 14.6 \times 10^{-3}$ $f_{I3} = 10.91$
Integrator on $C_{I1} = 1.46\ \mu F$	$T_{I1} = 1.872$ $f_{I1} = 0.08506$	$T_{I2} = 5.928$ $f_{I2} = 0.02686$	$T_{I3} \rightarrow \infty$ $f_{I3} \rightarrow 0$
0.4 BW Integrator off $A_I = 2.6 \times 10^6$	$T_{I1} = 1.482$ $f_{I1} = 0.1075$	$T_{I2} = 12.6 \times 10^{-3}$ $f_{I2} = 12.63$	$T_{I3} = 6.9 \times 10^{-3}$ $f_{I3} = 23.07$
Integrator on $C_{I1} = 0.69\ \mu F$	$T_{I1} = 1.482$ $f_{I1} = 1.075$	$T_{I2} = 3.276$ $f_{I2} = 0.04861$	$T_{I3} \rightarrow \infty$ $f_{I3} \rightarrow 0$
0.6 BW Integrator off $A_I = 2.6 \times 10^6$	$T_{I1} = 0.26$ $f_{I1} = 0.612$	$T_{2I} = 5.7 \times 10^{-3}$ $f_{2I} = 27.936$	$T_{3I} = 4.7 \times 10^{-3}$ $f_{3I} = 33.88$
Integrator on $C_{I1} = 0.47\ \mu F$	$T_{I1} = 0.26$ $f_{I1} = 0.612$	$T_{I2} = 1.482$ $f_{I2} = 9.306$	$T_{I3} \rightarrow \infty$ $f_{I3} \rightarrow 0$
High-speed preamplifier			
$A_p = 3.9 \times 10^6$	$T_{p1} = 0.159$ sec $f_{p1} = 1.00$ Hz	$T_{p2} = 1.602$ $f_{p2} = 0.0994$	
Final amplifier (low and high speed)			
$A_A = 1 \times 10^6$	$T_{1A} = 150 \times 10^{-3}$ $f_{1A} = 1.06$	$T_{2A} = 1.67$ $f_{2A} = 0.0965$	

Table 3. Results of simulation with normal motor gain

Case No.	Bandwidth setting	Gain setting	Percent overshoot	Delay time, sec	Rise time, sec	Settling time, sec	Noise bandwidth, Hz	3-dB Bandwidth, Hz	Phase margin, deg	Gain margin, dB
I	0.025	0	52.37	7.0	7.0	62.0	0.089	0.048	31.99	−18.18
II	0.05	5	77.09	4.0	4.0	62.5	0.310	0.089	16.3	−12.9

Table 4. Results of simulation with reduced motor gain

Case No.	Bandwidth setting	Gain setting	Percent overshoot	Delay time, s	Rise time, s	Settling time, s	Noise bandwidth, Hz	3-dB Bandwidth, Hz	Phase margin, deg	Gain margin, dB
III	0.025	0	51.93	24.0	30.0	326	0.021	0.011	31.6	−27.67
IV	0.05	5	63.83	12.0	13.5	191.	0.060	0.023	24.28	−10.80

Table 5. Test results from DSS 12

Bandwidth setting	Gain setting	Percent overshoot	Delay time, s	Rise time, s	Settling time, s	Noise bandwidth, Hz	3-dB Bandwidth, Hz	Phase margin, deg	Gain margin, dB
0.025	0	46	18.5	30.0	460	0.024	0.017	40.8	−16
0.05	5	40	8.6	10.4	91.5	0.05	0.026	39.3	−20.4

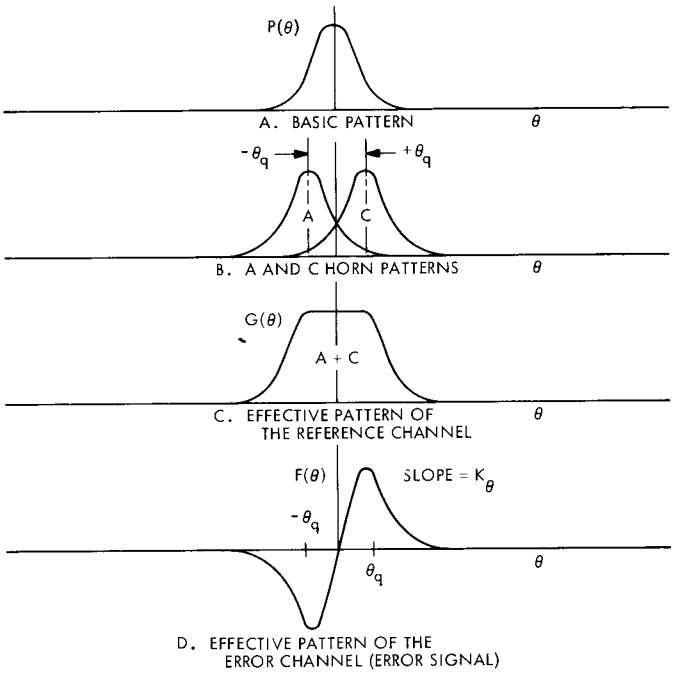

Fig. 1. Antenna and error patterns of the four-horn monopulse feed system

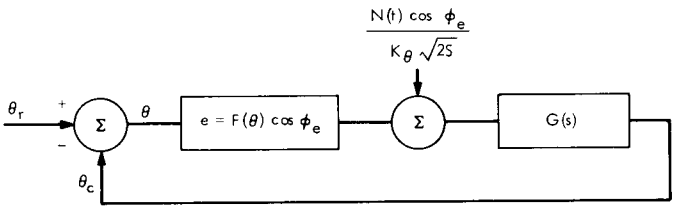

Fig. 2. System model of the automatic angle tracking system

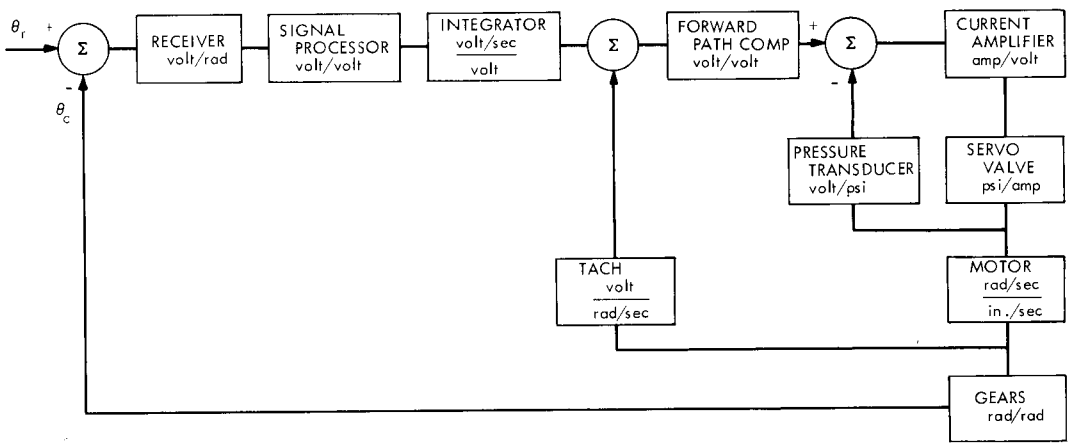

Fig. 3. Functional block diagram of the automatic angle tracking system

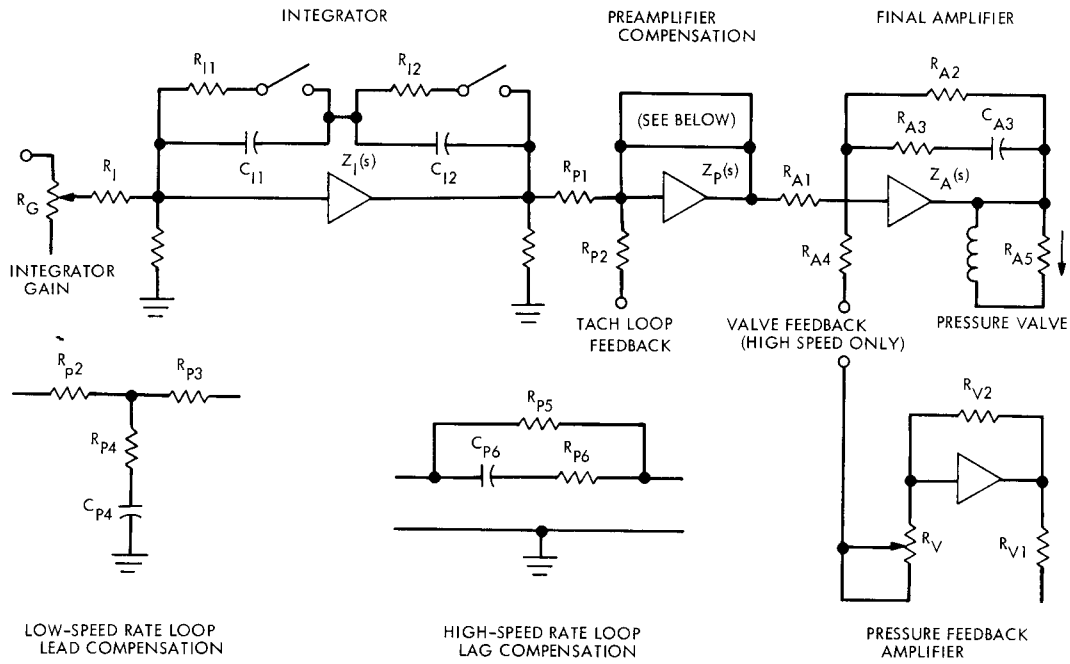

Fig. 4. Simplified schematic of the servo electronics

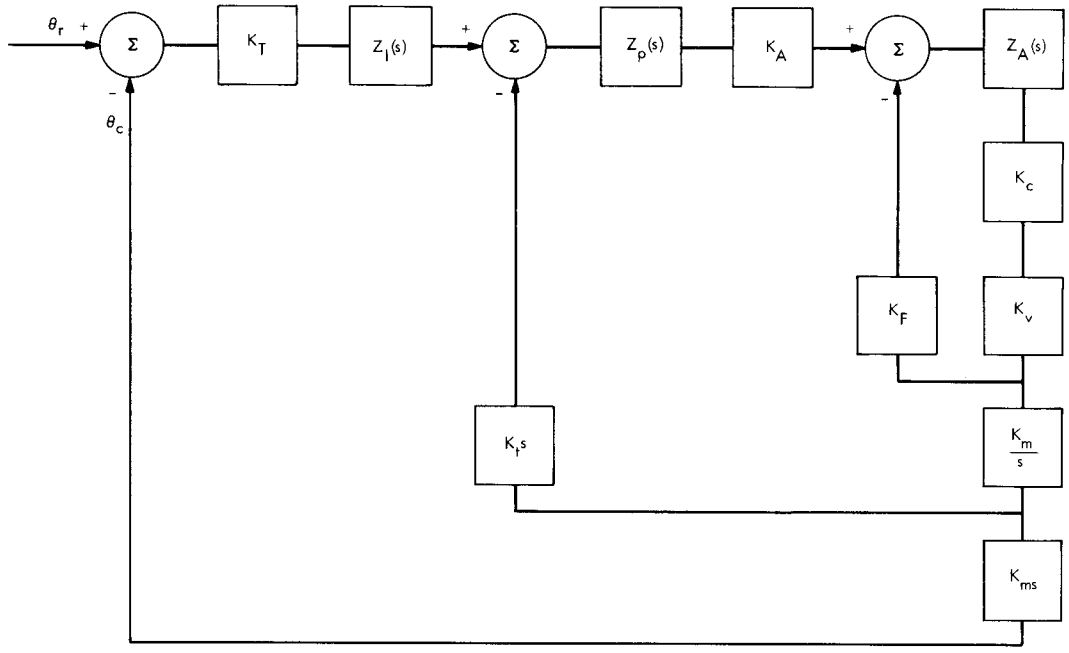

Fig. 5. Transfer function model of the automatic angle tracking system

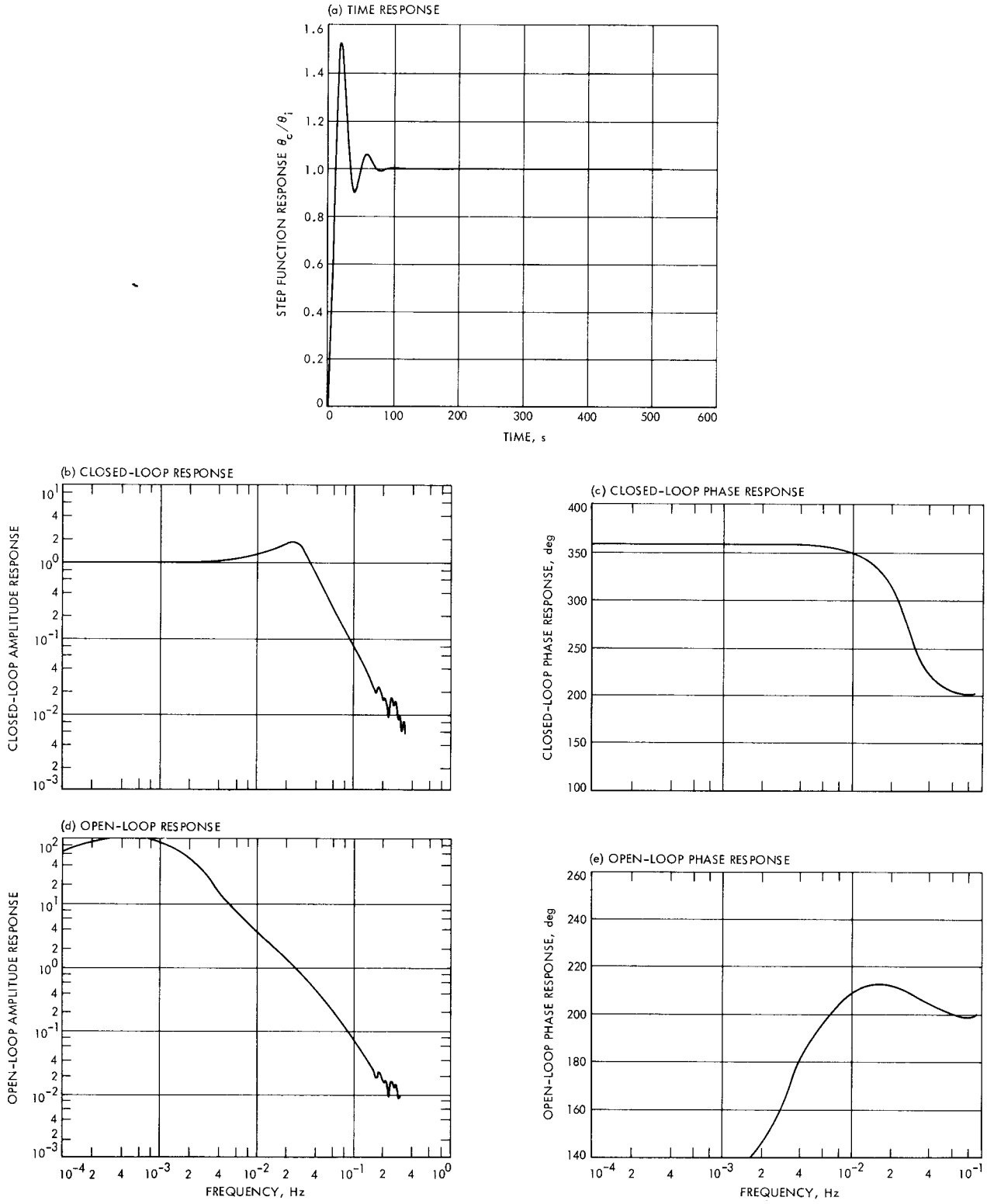

Fig. 6. Simulation results of case I (bandwidth = 0.025, gain setting = 0, normal motor gain): (a) time response, (b) closed-loop response, (c) closed-loop phase response, (d) open-loop response, (e) open-loop phase response

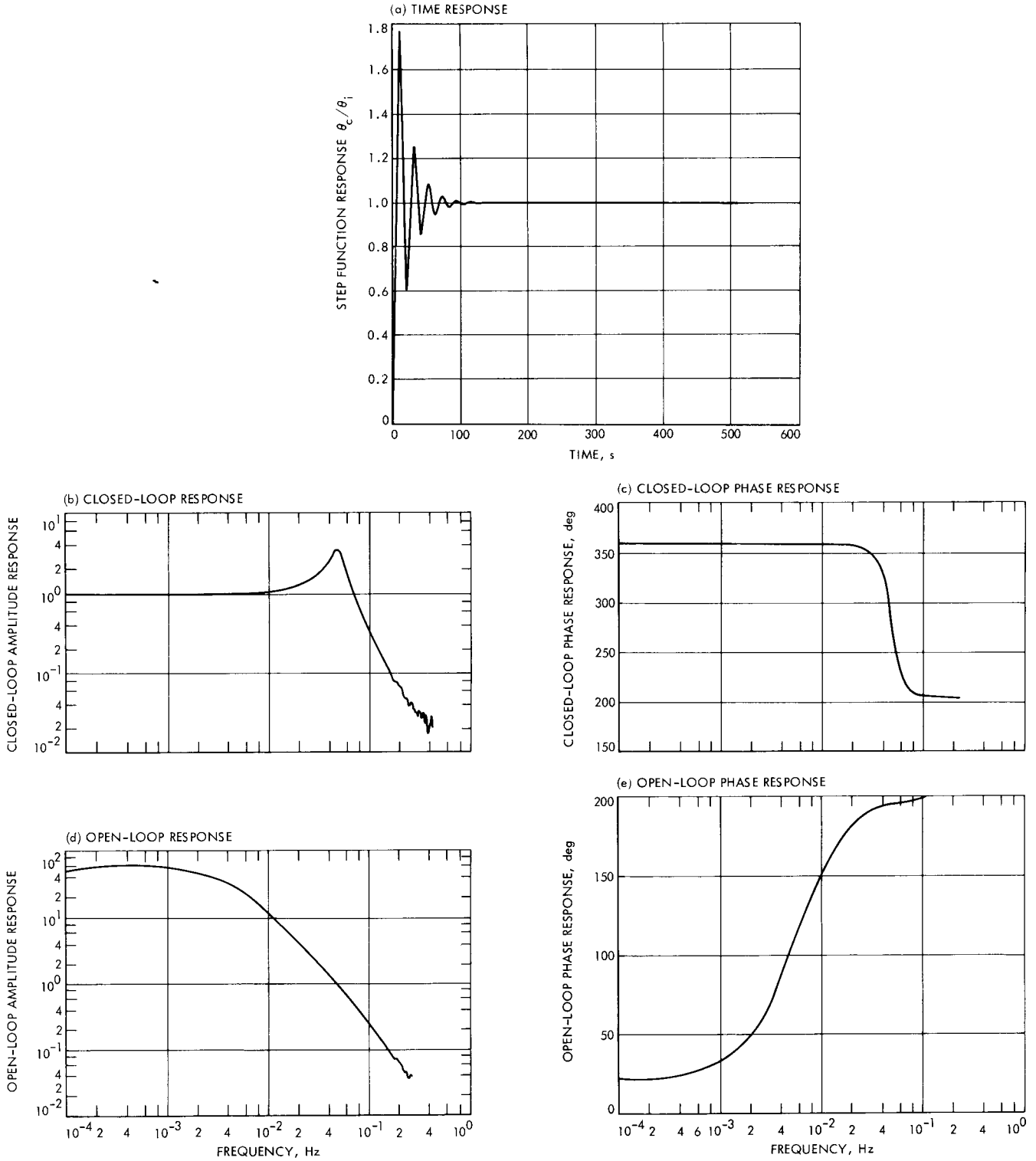

Fig. 7. Simulation results of case II (bandwidth = 0.05, gain setting = 5, normal motor gain): (a) time response, (b) closed-loop response, (c) closed-loop phase response, (d) open-loop response, (e) open-loop phase response

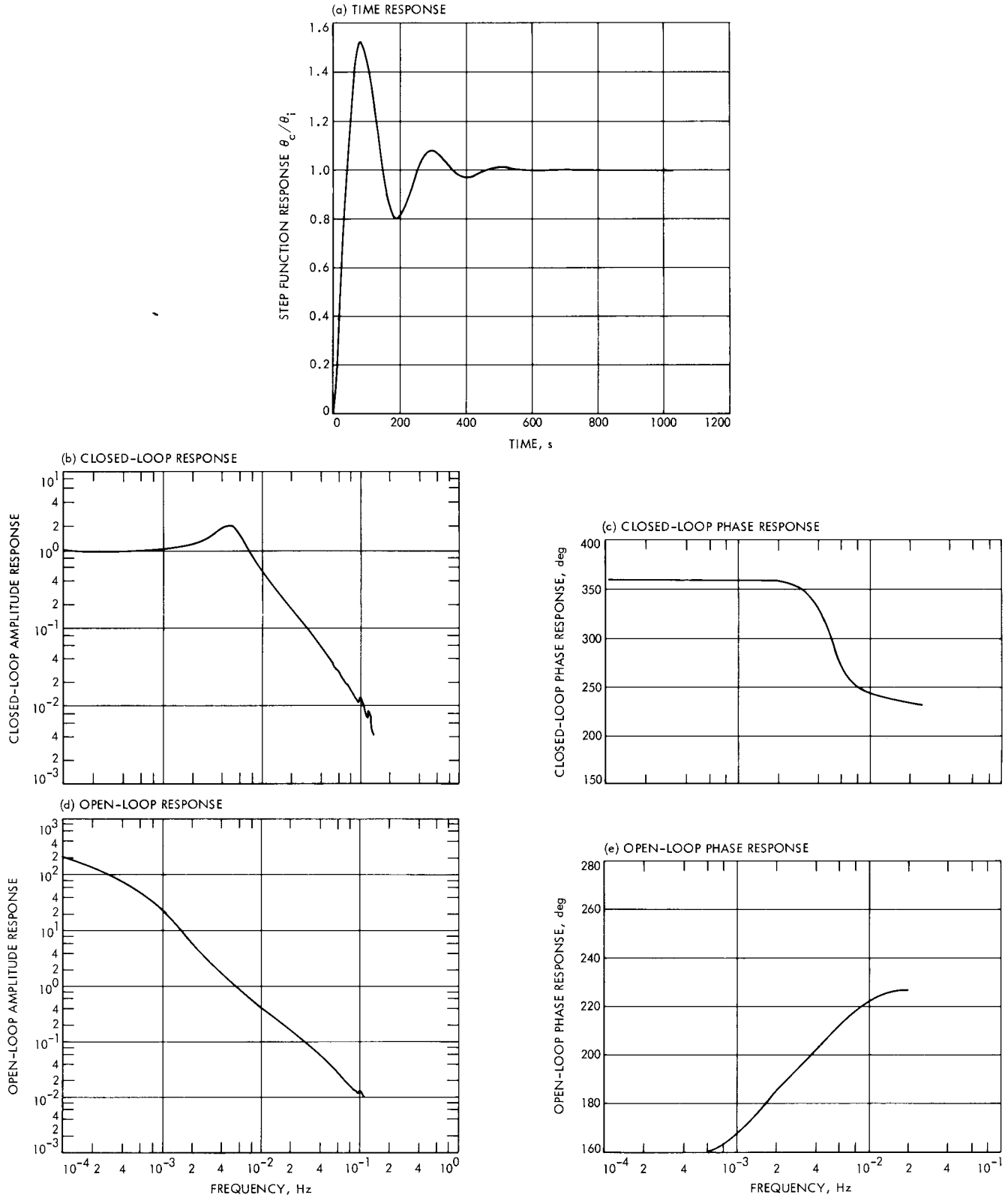

Fig. 8. Simulation results of case III (bandwidth = 0.024, gain setting = 0, reduced motor gain): (a) time response, (b) closed-loop response, (c) closed-loop phase response, (d) open-loop response, (e) open-loop phase response

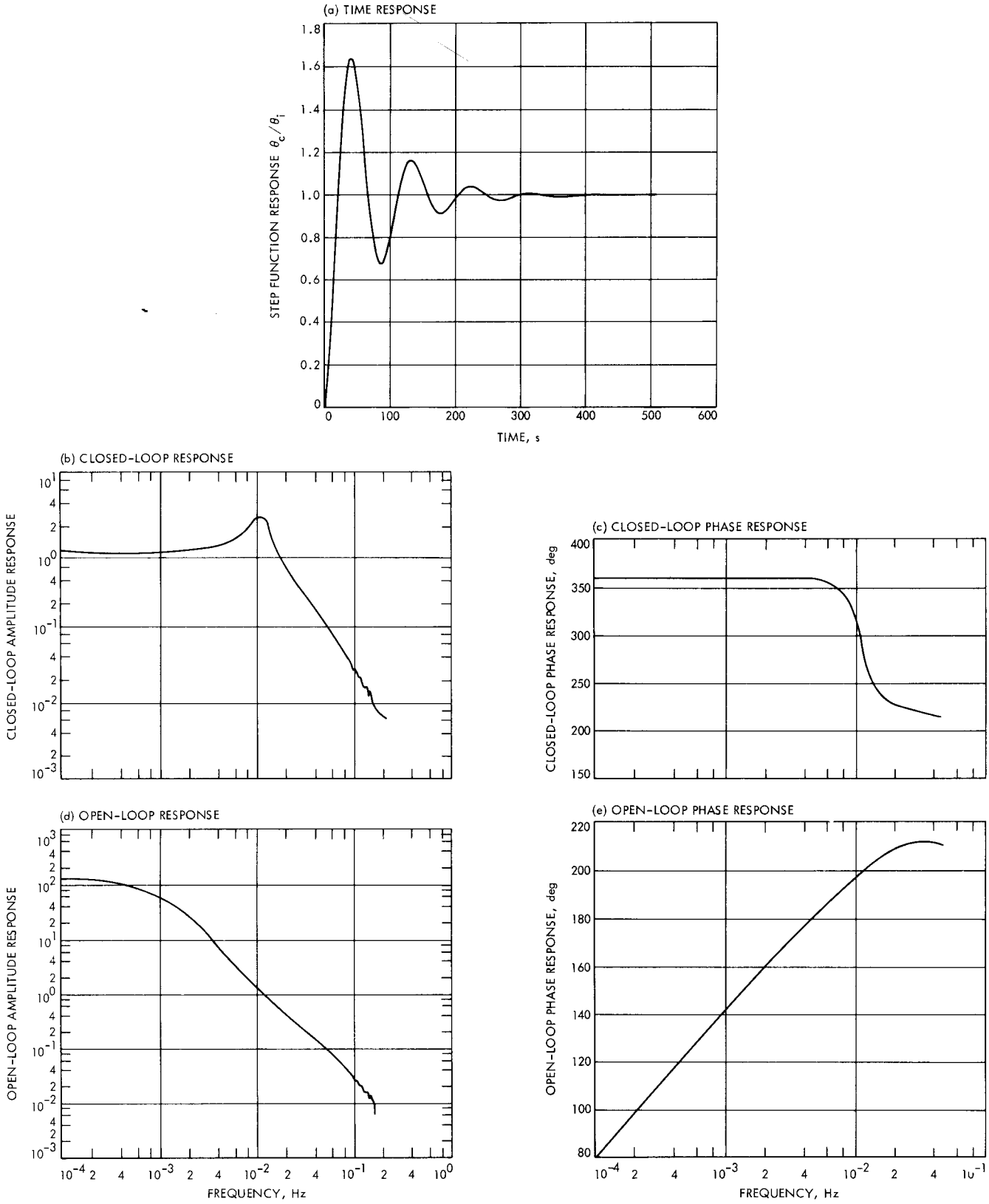

Fig. 9. Simulation results of case IV (bandwidth = 0.05, gainsetting = 5, reduced motor gain): (a) time response, (b) closed-loop response, (c) closed-loop phase response, (d) open-loop response, (e) open-loop phase response

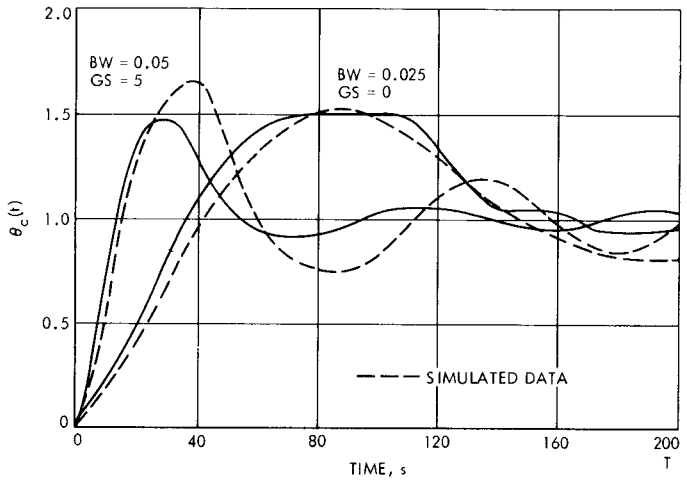

Fig. 10. Time responses measured at DSS 12

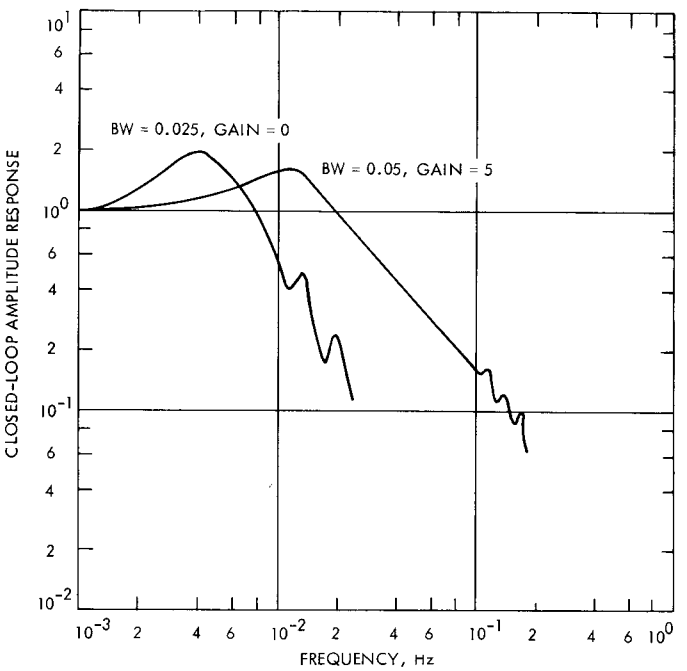

Fig. 11. Closed-loop transfer function measured at DSS 12